Title

Regulation of the fate of dental-derived mesenchymal stem cells using engineered alginate-GelMA hydrogels.

Journal

Journal of biomedical materials research. Part A, 105(11)

ISSN

1549-3296

Authors

Ansari, Sahar
Sarrion, Patricia
Hasani-Sadrabadi, Mohammad Mahdi
et al.

Publication Date

2017-11-01

DOI

10.1002/jbm.a.36148

Peer reviewed

HHS Public Access

Author manuscript

J Biomed Mater Res A. Author manuscript; available in PMC 2018 November 01.

Published in final edited form as:

J Biomed Mater Res A. 2017 November ; 105(11): 2957–2967. doi:10.1002/jbm.a.36148.

Regulation of the fate of dental-derived mesenchymal stem cells using engineered alginate-GelMA hydrogels

Sahar Ansari, MSc, PhD[1,#], **Patricia Sarrion, PhD**[1,#], **Mohammad Mahdi Hasani-Sadrabdi, PhD**[1,2], **Tara Aghaloo, DDS, MD, PhD**[3], **Benjamin M Wu, DDS, PhD**[1], and **Alireza Moshaverinia, DDS, MS, PhD**[1,*]

[1]Weintraub Center for Reconstructive Biotechnology, Division of Advanced Prosthodontics, School of Dentistry, University of California, Los Angeles, CA

[2]Parker H. Petit Institute for Bioengineering and Bioscience, G. W. Woodruff School of Mechanical Engineering and School of Materials Science and Engineering, Georgia Institute of Technology, Atlanta, GA, USA

[3]Division of Diagnostic and Surgical Sciences, School of Dentistry, University of California, Los Angeles, CA

Abstract

Mesenchymal stem cells (MSCs) derived from dental and orofacial tissues provide an alternative therapeutic option for craniofacial bone tissue regeneration. However, there is still a need to improve stem cell delivery vehicles to regulate the fate of the encapsulated MSCs for high quality tissue regeneration. Matrix elasticity plays a vital role in MSC fate determination. Here we have prepared various hydrogel formulations based on alginate and gelatin methacryloyl (GelMA) and have encapsulated gingival mesenchymal stem cells (GMSCs) and human bone marrow MSCs (hBMMSCs) within these fabricated hydrogels. We demonstrate that addition of the GelMA to alginate hydrogel reduces the elasticity of the hydrogel mixture. While presence of GelMA in an alginate-based scaffold significantly increased the viability of encapsulated MSCs, increasing the concentration of GelMA downregulated the osteogenic differentiation of encapsulated MSCs *in vitro* due to decrease in the stiffness of the hydrogel matrix. The osteogenic suppression was rescued by addition of a potent osteogenic growth factor such as rh-BMP-2. In contrast, MSCs encapsulated in alginate hydrogel without GelMA were successfully osteo-differentiated without the aid of additional growth factors, as confirmed by expression of osteogenic markers (Runx2 and OCN), as well as positive staining using Xylenol orange. Interestingly, after two weeks of osteo-differentiation, hBMMSCs and GMSCs encapsulated in alginate/GelMA hydrogels still expressed CD146, an MSC surface marker, while MSCs encapsulated in alginate hydrogel failed to express any positive staining. Altogether, our findings suggest that it is possible to control the fate of encapsulated MSCs within hydrogels by tuning the mechanical properties of the matrix. We also reconfirmed the important role of the presence of inductive signals in guiding MSC differentiation.

[*]Corresponding author: Alireza Moshaverinia, DDS, MS, PhD, FACP, Assistant Professor, Diplomate, American Board of Prosthodontics, Division of Advanced Prosthodontics, UCLA School of Dentistry, 10833 LeConte Ave, B3-023 CHS, Los Angeles, California 90095-1668, amoshaverinia@ucla.edu, Tel: (310) 794-6324.

[#]These authors contributed equally to this work.

These findings may enable the design of new multifunctional scaffolds for spatial and temporal control over the fate and function of stem cells even post-transplantation.

Keywords

alginate hydrogel; GelMA; biomaterials; elasticity; bone tissue engineering

Introduction

Mesenchymal stem cells (MSCs) are considered to be advantageous alternative therapeutic option for bone tissue engineering. The use of culture-expanded MSCs in conjunction with hydrogel biomaterials has been widely reported for clinical applications in bone regeneration and repair. [1-3] Stem cell delivery vehicles have a crucial role in the performance of encapsulated cells and the success of the regenerative therapies. [1-5] Hydrogel biomaterials are extensively utilized to engineer and mimic the physiochemical properties of the extracellular stem cell microenvironment to mimic niche characteristics and regulate cell phenotype and differentiation. 2D and 3D scaffolds have been largely used to study stem cell-biomaterial interactions by encapsulating stem cells within hydrogel biomaterials. [6-8] Hydrogel biomaterials provide a 3D biomaterial platform for engineering stem cell niches for different tissue engineering applications. Studies have shown that the architectural features of the hydrogel niche, as the encapsulating biomaterial, can control the quiescence and fate of stem cells. The fate of the encapsulated stem cells is regulated by hydrogel mechanical properties such as stiffness and elasticity. [9-11] Additionally, it is well documented that inductive signals direct the differentiation of stem cells toward a desired lineage.[4-9] In order to develop effective stem cell-mediated regenerative therapies, it is vital to take advantage of a biomaterial with proper mechanical properties and a versatile microarchitecture that promotes cell binding and viability. Several types of biomaterials have been used as 3D delivery vehicles for MSCs. Among these, alginate hydrogel is one of the popular choices.[12-15] Alginate hydrogel is a natural polymer derived from brown sea algae. It is a heteropolysaccharide composed of (1-4)-linked b-D-mannuronic acid and a-L-guluronic acid.[12-16] Sodium alginate ionically crosslinks in the presence of divalent cations (e.g. Ca^{2+}). [14-16] Alginate has found a wide variety of biomedical applications due to its favorable characteristics, such as biocompatibility, non-toxicity, and gentle gelation. For these reasons, the US Food and Drug Administration (FDA) have approved alginate for a number of clinical trials.[13-15] Additionally, alginate scaffolds are frequently used for drug delivery applications. Alginate as an encapsulating biomaterial has favorable mechanical properties and maintains excellent cell viability.[17] However, it lacks binding properties to cells and shows lower biodegradability in the presence of encapsulated stem cells. The absence of cell adhesion properties significantly restricts the cell ability to proliferate, elongate, migrate and organize into higher order structures.[17] Therefore, the structure of alginate hydrogel has been modified with binding motifs such as Arg-Gly-Asp (RGD) to imitate the natural composition of the extracellular matrix (ECM). [18,19] In addition to RGD groups, matrix metalloproteinase (MMP)-sensitive degradation sequences have been added to the structure of alginate hydrogel formulations to expedite degradation profile and have exhibited promising outcomes in several biomedical applications.[20,21] Studies have

confirmed that alginate hydrogels can be used successfully to direct differentiation of encapsulated mesenchymal stem cells (MSCs) toward desired lineage phenotypes. [17-19]

Another hydrogel biomaterial that is a promising scaffold for stem cells is gelatin methacrylate (GelMA), which is a photocrosslinkable hydrogel biomaterial comprised of modified natural ECM components. Gelatin is derived from inexpensive, denatured collagen, which contains integrin binding motifs and matrix metalloprotein (MMP) degradation sites. [22,23] Like alginates, GelMA has been used extensively as a cell delivery vehicle for biomedical applications. [22-25]

For successful application in promoting high quality tissue regeneration, a hydrogel biomaterial should possess biomechanical properties similar to those of the natural ECM to provide an optimal environment for the growth and differentiation of encapsulated cells toward the desired phenotype. We hypothesized that a hydrogel biomaterial composed of alginate and GelMA could be used successfully as cell-laden hydrogel biomaterial with tunable mechanical properties for directing the fate of encapsulated MSCs. Therefore, in the current study, we sought to engineer an alginate-GelMA hydrogel as an MSC microenvironment in order to tailor the niche characteristics and direct the encapsulated stem cells through osteogenic differentiation.

2. Materials and methods

2.1. Stem cell isolation and culture

Young healthy male individuals undergoing third molar extractions were chosen for extraction of gingival tissues (with related IRB approval). GMSCs were isolated and cultured according to published protocols. [19,26] As the control group, human bone marrow (hBM) MSCs (Lonza Inc. Walkersville, MD), were used. In order to ensure that MSCs were positive for MSC surface markers STRO-1 and CD146 (BD Biosciences, San Jose, CA), flow cytometric examination was used. Passage 4 cells were used in all the experiments.

2.2. Biomaterial fabrication and cell encapsulation

High molecular weight alginate was purchased from NovaMatrix, Norway. The hydrogel biomaterial was charcoal treated, oxidized (2%) using sodium periodate (Sigma, St. Louis, MO), and sterile filtered (0.22 μm filters, Millipore, Billerica, MA) prior to the cell encapsulation process. Alginate solution (3 w/v%) was prepared by dissolving freeze-dried alginate in PBS.

GelMA (derived from porcine skin gelatin) was synthesized as previously described. [22, 23] Next, GelMA solution was prepared by dissolving the freeze-dried GelMA (1 w/v%) and the photoinitiator (Irgacure 2959, 0.25 w/v%; Sigma-Aldrich) in PBS. Subsequently, alginate and GelMA solutions with two different concentrations of alginate: GelMA were made: 3:1 (w/v%: w/v%) and 1:1 (w/v%: w/v%) (Figure 1a). Alginate hydrogel alone was used as the control scaffold.

1×10^6 hBMMSCs or GMSCs were encapsulated in 1 mL of each alginate/GelMA hydrogel formulation or alginate hydrogel. Microsphere formation was accomplished by adding

alginate-based droplets (10μl) dropwise into a 100 mM $CaCl_2$ solution. A secondary crosslinking was performed by UV crosslinking for 15 seconds using OmniCure S2000 UV lamp (Lumen Dynamics, Ontario, Canada). Cell-free alginate/GelMA or alginate hydrogel specimens were used as the negative control.

2.3. Measurement of viability of encapsulated MSCs

In order to evaluate the viability of the encapsulated MSCs a live-dead assay (Calcein AM/ ethidium bromide homodimer-1, Invitrogen) was utilized for up to two weeks after culturing in regular culture media according to published protocols.[15,16] NIH ImageJ software (NIH, Bethesda, MD) was used to quantify the percentage of live cells.

2.4. Characterization of the alginate/HA hydrogels

The biomechanical properties of the prepared hydrogels with different alginate/GelMA ratios were measured and the elastic modulus (E) of each preparation was calculated using atomic force microscopy (AFM)-assisted nanoindentation (Bruker Dimension Icon) at a rate of 3 μm.s^{-1} with the trigger force of 2 nN according to methods in the literature.[27] Elastic modulus (E) was calculated using Hertz contact model for the spherical elastic solid. Poisson ratio (v) of 0.5 fit over a range of 10 to 90% indentation force.

Moreover, the morphology and pore sizes of the fabricated hydrogels were analyzed using scanning electron microscopy (SEM) (Zeiss Supra 40VP). To assess the swelling kinetics of the fabricated microspheres, the microspheres were immersed into the distilled water at 37°C after incubation for 45 min for completion of crosslinking. Afterwards, at time intervals up to 10 h, the weight of each swollen specimen was measured after the removal of the excess surface solution using a filter paper. The swelling ratio (SR) was calculated according to the formula below:

$$SR = \frac{w_t - w_o}{w_o}$$

where W_t and W_o are the weight of the swollen hydrogel at time t and the weight of the unswollen hydrogel on day 0, respectively.

2.5. *In vitro* osteo-differentiation of encapsulated MSCs

Encapsulated hBMMSCs and GMSCs were cultured in osteogenic media containing a-MEM, 10 % FBS, 1 % penicillin, streptomycin, and dexamethasone (0.1 mM), b-glycerophosphate (10 mM), and ascorbic acid (50 mg/ml). and 1.8 mM potassium dihydrogen phosphate (Sigma). Encapsulated MSCs were cultured for 4 weeks in the osteogenic media. Next, the specimens were retrieved and stained with Alizarin red and Xylenol orange (XO). Furthermore, the expression of Runx2 and OCN was analyzed using q-PCR assay. Cell-free alginate/GelMA microspheres were used as the negative control.

Additionally, in another set of osteogenic induction assay, encapsulated MSCs were grown in the regular culture media containing 25μg/mL of rh-BMP2 (Medtronic) and after four weeks the osteogenesis was analyzed using gene expression and XO staining.

2.6. Quantitative real-time PCR assay

Encapsulated MSCs were recovered from hydrogel microspheres after four weeks of osteogenic induction and total RNA was isolated using Trizol reagent (Invitrogen). RNA was reverse-transcribed and single-stranded cDNA was synthesized using a Superscript III cDNA synthesis kit (Invitrogen). Relative gene expression was calculated using the $2^{-\Delta\Delta Ct}$ method, with normalization to the Ct of the housekeeping gene GAPDH (glyceraldehyde 3-phosphate dehydrogenase). Table 1 describes the primer sequences used on this study.

2.7. Immunofluorescence staining

In order to identify the stemness of encapsulated MSCs in different hydrogel formulations, immunoflurescence staining was performed using anti-CD146 antibody (Abcam). Briefly, after two weeks of culturing in osteogenic media, the specimens were retrieved, PFA (4%) fixed, paraffin embedded, sectioned (6 μm), and deparaffinized. The slides were treated with 3% H_2O_2 and then with a blocking buffer (1% BSA and 0.25% Triton X-100 in PBS) and stained with CD146 primary antibody (1:200, Abcam) over night. Next, secondary Alexa-Fluor conjugated goat anti-mouse IgG (1:200, Invitrogen) was used and specimens were counterstained with DAPI (Vector Laboratories, Burlingame, CA).

2.8. Statistical Analysis

Quantitative data were expressed as mean and standard deviation (SD). One-way and two-way analyses of variance, followed by Tukey's test at a significance level of $\alpha = 0.05$, were used for comparison among multiple sample means. If necessary, the data were analyzed using Student's t-tests.

3. Results

3.1. Viability of encapsulated cells in alginate/GelMA hydrogels

In the current study, GMSCs were isolated from gingival tissues of patients with healthy periodontium. The isolated GMSCs were expanded *in vitro*, encapsulated in one of the fabricated alginate/GelMA hydrogels and utilized in *in vitro* osteo-differentiation assays. Human BMMSCs were used as the positive control, while cell-free hydrogels were used as the negative one. Additionally, the expression of specific MSC surface markers such as STRO-1 and CD-146 was analyzed using flow cytometric analysis, which confirmed the stemness of the MSCs (supplementary Figure 1).

In this study, the fabricated alginate and alginate/GelMA microspheres had an average diameter of 1 mm ± 0.12 (Figure 1b). The microscopic images of MSC- loaded hydrogels demonstrated that they exhibited a uniform size and stem cell distribution (Figure 1b). In the next step, the viability of the encapsulated GMSCs and hBMMSCs was assessed. MSCs were encapsulated in the hydrogels at a cell density of 1×10^6 cells/mL and the viability of MSCs was measured after 1, 7 and 14 days of culturing. Our live/dead staining results demonstrated high *in vitro* viability for encapsulated GMSCs and hBMMSCs cultured in regular culture media at all tested time intervals (Figure 1c-1f). Interestingly, the viability of encapsulated MSCs increased as the percentages of GelMA increased in the fabricated

hydrogels ($p>0.05$), which might be related to the presence of cell binding motifs in GelMA hydrogels.

3.2. Characterization of fabricated hydrogels

SEM analysis was utilized to assess the morphological structure of the fabricated hydrogels and our data confirmed a porous morphology (Figure 2a-2d). Additionally, our SEM analysis showed that the percentage of GelMA in the structure of the fabricated hydrogels affected the porosity (Figure 2e). Alginate/GelMA hydrogels with 1:1 w/w ratio showed a significantly greater percentage of porosity in comparison to alginate alone or Alginate/GelMA hydrogel with a 3:1 ratio (Figure 2e).

Moreover, we assessed the influence of the composition of the hydrogels on the swelling ratio (Figure 1f). Diffusion of penetrant molecules in to the free volume of hydrogel network and subsequent polymer relaxation are known as the two molecular processes of swelling (35). Here by simple logarithmic fitting of the swilling kinetic data to the swelling rate equation $SR= kt^n$, we have tried to dig deeper into changes in the molecular structure of alginate-based hydrogels in the presence of GelMA chains. It has to be mentioned that in the swelling rate equation, k is the gel characteristic constant while n is the kinetic exponent. In this phenomenological law equation, n is related to the type of sorption mechanisms of hydrogels, which can be divided into three states: n=0.5 will demonstrate the Fickian kinetics, where the rate of water diffusion is the limiting factor ($0<n<0.5$ represents "less Fickian" diffusion). When n=1, the rate of water diffusion is far greater than the chain stretching/relaxation rate, therefore, the water uptake is proportional to the time; $0.5<n<11$; this represents a non-Fickian process.

Linear fitting of $log_{10}(SR)$ vs. $log_{10}(t)$ was used to determine n values (Figure 1g). The values of n for alginate, alginate/GelMA (1:1) and alginate/GelMA (3:1) hydrogels were 0.65, 0.51, and 0.38 (Figure 1h), respectively. An increase in the composition of GelMA results in the prohibition of well-structured electrostatic interactions between alginate's carboxylic acid groups and Ca^{2+} ions, leading to chain expansion, which increases the macromolecular chain relaxation rate ($Rate_{diffusion} \ll Rate_{relaxation}$). Thus, the swelling mechanism becomes more diffusion-controlled in the presence of GelMA chain, and n values decrease.

It is well known that the elastic modulus of the matrix plays a role in directing the fate of encapsulated cells [53]. Therefore, we fabricated and tested two different hydrogels with different alginate/GelMA ratios (1:1 and 3:1 w/w) and compared them to alginate hydrogel without GelMA. Subsequently, the mechanical properties of the fabricated hydrogels were characterized. The data exhibited in Figure 1i-j show the elastic modulus of the fabricated hydrogels with different compositions. The formulation with the highest concentration of GelMA (Alg/GelMA: 1:1) exhibited the lowest elastic modulus (6 kPa) of the three tested hydrogels. Alginate hydrogel alone showed the greatest elasticity (13 kPa). The mechanical properties of the hydrogels are in accordance with the predicted relaxation of the hydrogels based on the swelling kinetics.

3.3. In vitro osteogenic differentiation assay

An in vitro osteogenic differentiation assay was utilized to evaluate the effect of the composition and properties of the encapsulating hydrogel biomaterial on the osteo-differentiation potential of encapsulated GMSCs and hBMMSCs. 1×10^6 GMSCs or hBMMSCs were encapsulated in 1 ml alginate, alginate/GelMA (1:1) or alginate/GelMA (3:1) hydrogels and the fabricated microspheres were cultured in osteogenic media containing dexamethasone, l-ascorbate-2-phosphate, and phosphate. After 4 weeks of osteo-differentiation, both of the examined MSCs exhibited positive XO labeling (Fig. 3a, b). However, MSCs encapsulated in alginate/GelMA hydrogels showed significantly less amounts of mineralization in comparison to MSCs encapsulated in alginate hydrogel alone ($p<0.05$). Moreover, an increase in the amount of GelMA in the composition of the hydrogel further decreased the mineralization ($p>0.05$) (Figure 3).

Gene expression analysis was performed to evaluate the molecular mechanism of osteo-differentiation of encapsulated MSCs. *Runx2* and *OCN* expression levels were analyzed (Figure 4). Our quantitative PCR analysis showed that GMSCs and hBMMSCs encapsulated in alginate hydrogel abundantly expressed *Runx2* and *OCN* four weeks after *in vitro* differentiation (Figure 4). However, our quantitative analysis of gene expression demonstrated that GMSCs and hBMMSCs encapsulated in alginate/GelMA hydrogels showed significantly lower expression levels of genes associated with osteogenic differentiation than MSCs encapsulated in alginate alone ($p < 0.05$) (Figure 4). Moreover, encapsulated cells in the hydrogel with the lowest modulus of elasticity (Alg/GelMA 1:1) showed statistically lower ($p < 0.05$) levels of osteogenic-related gene expression than MSCs encapsulated in a matrix with higher elasticity. These data prompted us to analyze the specimens for adipogenic-related genes to assess whether the lower modulus of elasticity of alginate/GelMA directs the fate of encapsulated MSCs toward adipogenesis. However, our qPCR analysis failed to show expression of genes related to adipogenic differentiation such as *Peroxisome proliferators activated receptor-γ2* (*PPAR-γ2*) and *lipoprotein lipase* (*LPL*) (supplementary Figure 2). Additionally, Oil O red stationing failed to present any positive staining (data not shown).

These data prompted us to examine the ability of alginate/GelMA hydrogel formulation to function as a niche for MSCs to keep their stemness properties *via* immunofluorescence staining against CD146 antibodies. Interestingly, hBMMSCs and GMSCs encapsulated in alginate/GelMA hydrogels still expressed CD146, an MSC surface marker, while MSCs encapsulated in alginate hydrogel failed to express any positive staining. Moreover, encapsulated MSCs in hydrogel compositions with greater amounts of GelMA exhibited an increased amount of CD146 expression (Figure 5).

Next, in order to analyze the importance of the presence of signaling molecules in the microenvironment, 1×10^6 hBMMSCs were encapsulated in 1 ml alginate, alginate/GelMA (1:1) or alginate/GelMA (3:1) hydrogels and the fabricated microspheres were cultured in regular media containing rh-BMP2, a potent osteogenic growth factor. After four weeks of osteo-differentiation, Alizarin red and XO fluorescence staining showed significant positive staining of hBMMSCs encapsulated in alginate/GelMA hydrogels (Figure 6). Our results confirmed that rhBMP2 can rescue the osteogenesis of encapsulated MSC in alginate/

GelMA hydrogels (Figure 6). The specimens cultured in the presence of rh-BMP2 failed to express positive CD146 staining.

4. Discussion

Recently, we showed that RGD- coupled alginate hydrogels are promising scaffolds for encapsulation of hBMMSCs or dental-derived MSCs such as GMSCs. Additionally, we have reported that modification of alginate hydrogels with RGD tripeptide significantly increased stem cell adhesion, viability, and osteogenic differentiation capacity.[15, 16, 19, 33, 34] In the current study, we showed that MSCs encapsulated in all the fabricated alginate-GelMA hydrogels maintained high cell viability up to two weeks, which confirms that oxygen and nutrients that could reach the cell cluster within the hydrogel spheres. These findings are attributed to the small size of microspheres and their porous microstructure. Moreover, the encapsulated hBMMSCs and GMSCs continued to present their undifferentiated state as single-cell suspensions. Additionally, it was shown that presence of GelMA in the structure of the encapsulating hydrogel increased the percentage of viable MSCs, which suggests the presence of cell binding motifs plays an important role in maintaining the viability of the encapsulated MSCs.

Studies have shown that the differentiation capacity of stem cells can be regulated by the physiomechanical properties of scaffold biomaterials, such as their porosity and polymer concentration.[30] Additionally, it has been reported that cell biomaterial interactions play vital roles in controlling stem cell apoptosis, quiescence, self-renewal, and differentiation. [9, 11, 31] For instance, it has been reported that the presence of cell binding motifs (e.g., RGD) can control critical cell functions such as differentiation and proliferation.[32] The stem cell niche plays a vital role in the maintenance of the quiescent (undifferentiated) state of stem cells and in their differentiation toward desired lineages. Specifically for adult stem cells (e.g., hBMMSCs or GMSCs), the niche supports quiescence to maintain their long-term regeneration capability. [28,29]

Our *in vitro* osteogenic differentiation assay showed that hBMMSCs and GMSCs encapsulated in alginate/GelMA hydrogels (with 1:1 or 3:1 weight ratios) exhibited very modest levels of positive xylenol orange staining and expression of osteogenic related genes such as *Runx2* and *OCN*. These findings may be explained by the lower elastic modulus of alginate/GelMA hydrogels in comparison to alginate without GelMA. Interestingly, the hydrogel mixture with a greater amount of GelMA in its structure showed a decreased expression of osteogenic-related genes and lower amounts of XO staining.

Our findings in the current study, demonstrate that the addition of the GelMA to alginate made the fabricated hydrogel less favorable for differentiation of encapsulated MSCs toward osteogenic lineage, which is attributed to the decrease in the elasticity of the biomaterial. Therefore, considering the elasticity of the developed hydrogel, we assessed the suitability of alginate/GelMA hydrogel for adipogenic differentiation of encapsulated MSCs. However, our qPCR analysis failed to show expression of genes related to adipogenic differentiation such as *Peroxisome proliferators activated receptor-γ2* (*PPAR-γ2*) and *lipoprotein lipase* (*LPL*). These data prompted us to examine the capability of alginate/GelMA hydrogel to act

as a niche for MSCs to keep their stemness properties. Interestingly, hBMMSCs and GMSCs encapsulated in alginate/GelMA hydrogels still expressed CD146, an MSC surface marker, while MSCs encapsulated in alginate hydrogel failed to express any CD146-positive staining. Moreover, encapsulated MSCs in hydrogel compositions with greater amounts of GelMA exhibited an increased amount of CD146 expression. These data confirmed the important role of the matrix in determining the quiescence and fate of encapsulated stem cells.

In order to evaluate the regulatory effect of the presence of signaling molecules in the fate determination of encapsulated MSCs, the encapsulated MSCs were cultured in regular media containing rh-BMP2, a potent osteogenic growth factor. Our data clearly showed that rh-BMP2 can rescue the osteogenesis of encapsulated MSCs in alginate/GelMA hydrogels. Our data highlight the significance of engineering the appropriate microenvironment for stem cells with optimized mechanical properties and cell binding motifs. We also confirmed the importance of presentation of the inductive signals for osteo-differentiation of MSCs for high quality tissue regeneration.

Altogether, our findings in the current study confirm that differentiation capacity of encapsulated MSCs is regulated by the physiochemical properties of the hydrogel biomaterial, as well as the presence of inductive signals. These parameters will determine the fate of encapsulated MSCs toward the desired phenotype.

5. Conclusions

This study describes a bone regeneration strategy based on *in vitro* experiments demonstrating the capacity of GMSCs and hBMMSCs to respond to the matrix physic-chemical properties and provided inductive signals. Altogether, our findings suggest that it is possible to control the fate of encapsulated MSCs within hydrogels by tuning the hydrogel matrix mechanical properties (e.g. elasticity) and the level of cell-matrix interactions. We also confirmed the value of presenting inductive signals for osteo-differentiation of MSCs for high quality tissue regeneration. These findings may enable the design of new multifunctional scaffolds for spatial and temporal control over the fate and function of stem cells even post-transplantation.

Supplementary Material

Refer to Web version on PubMed Central for supplementary material.

Acknowledgments

Authors (S.A. and A.M.) would like to thank Prof. Ali Khademhosseini for his critical review of the manuscript. This work was supported by a grant from the National Institute of Dental and Craniofacial Research, National Institutes of Health (DE023825 to A.M.).

References

1. Liu J, Sato C, Cerletti M, Wagers A. Notch signaling in the regulation of stem cell self-renewal and differentiation. Curr Top Dev Biol. 2010; 92:367–409. [PubMed: 20816402]

2. Kratchmarova I, Blagoev B, Haack-Sorensen M, Kassem M, Mann M. Mechanism of divergent growth factor effects in mesenchymal stem cell differentiation. Science. 2005; 308:1472–7. [PubMed: 15933201]

3. Moshaverinia A, Chen C, Xu X, Ansari S, Zadeh HH, Schricker SR, et al. Regulation of the Stem Cell-Host Immune System Interplay Using Hydrogel Coencapsulation System with an Antiinflammatory Drug. Adv Func Mater. 2015; 15:2296–2307.

4. Cantu DA, Hematti P, Kao WJ. Cell encapsulating biomaterial regulates mesenchymal stromal/stem cell differentiation and macrophage immunophenotype. Stem Cells Transl Med. 2012; 1:740–9. [PubMed: 23197666]

5. Czyz J, Wobus AM. Embryonic stem cell differentiation: the role of extracellular factors. Differentiation. 2001; 68:167–74. [PubMed: 11776469]

6. Tolar J, Le Blanc K, Keating A, Blazar BR. Concise review: hitting the right spot with mesenchymal stromal cells. Stem Cells. 2010; 28:1446–1455. [PubMed: 20597105]

7. Panetta NJ, Gupta DM, Quarto N, Longaker MT. Mesenchymal cells for skeletal tissue engineering. Panminerva Med. 2009; 51:25–41. [PubMed: 19352307]

8. Benfenati V, Pistone A, Sagnella A, Stahl K, Camassa L, Gomis-Perez C, Toffanin S, Torp R, Kaplan DL, Ruani G, Omenetto FG, Zamboni R, Muccini M. Silk fibroin films are a bio-active interface for neuroregenerative medicine. J Appl Biomater Function Mater. 2012; 10:315–323.

9. Discher DE, Mooney DJ, Zandstra PW. Growth factors, matrices, and forces combine and control stem cells. Science. 2009; 324:1673. [PubMed: 19556500]

10. Peerani R, Zandstra PW. Enabling stem cell therapies through synthetic stem cell-niche engineering. J Clin Invest. 2010; 120:60–70. [PubMed: 20051637]

11. Reilly GC, Engler AJ. Intrinsic extracellular matrix properties regulate stem cell differentiation. J Biomech. 2010; 43:55–62. [PubMed: 19800626]

12. Drury JL, Dennis RG, Mooney DJ. The tensile properties of alginate hydrogels. Biomaterials. 2004; 25:3187–3199. [PubMed: 14980414]

13. Smidsrod O, Skjakbraek G. Alginate as immobilization matrix for cells. Trends in biotechnology. 1990; 8:71–78. [PubMed: 1366500]

14. Alsberg A, Anderson KW, Albeiruti A, Franceschi RT, Mooney DJ. Cell-interactive Alginate Hydrogels for Bone Tissue Engineering. J Dent Res. 2001; 80:2025–2029. [PubMed: 11759015]

15. Moshaverinia A, Chen C, Akiyama K, Ansari S, Xu X, Chee WW, Schricker SR, Shi S. Alginate hydrogel as a promising scaffold for dental-derived stem cells: an in vitro study. J Mater Sci: Mater Med. 2012; 23:3041–3051. [PubMed: 22945383]

16. Moshaverinia A, Chen C, Akiyama K, Xu X, Chee WW, Schricker SR, Shi S. Encapsulated dental-derived mesenchymal stem cells in an injectable and biodegradable scaffold for applications in bone tissue engineering. J Biomed Mater Res A. 2013; 101:3285–94. [PubMed: 23983201]

17. Lee KY, Mooney DJ. Alginate: properties and biomedical applications. Prog Polym Sci. 2012; 37:106–126. [PubMed: 22125349]

18. Markusen JF, Mason C, Hull DA, Town MA, Tabor AB, Clements M, Boshoff CH, Dunnill P. Behavior of adult human mesenchymal stem cells entrapped in alginate-GRGDY beads. Tissue Eng Part A. 2006; 12:821.

19. Moshaverinia A, Chen C, Xu X, Akiyama K, Ansari S, Zadeh HH, Shi S. Bone regeneration potential of stem cells derived from periodontal ligament or gingival tissue sources encapsulated in RGD-modified alginate scaffold. Tissue Eng Part A. 2014; 20:611–21. [PubMed: 24070211]

20. Kraehenbuehl TP, Zammaretti P, Van der Vlies AJ, Schoenmakers RG, Lutolf MP, Jaconi ME, et al. Three-dimensional extracellular matrix-directed cardioprogenitor differentiation: systematic modulation of a synthetic cell- responsive PEG-hydrogel. Biomaterials. 2008; 29:2757–2766. [PubMed: 18396331]

21. Seliktar D, Zisch AH, Lutolf MP, Wrana JL, Hubbell JA. MMP-2 sensitive, VEGF- bearing bioactive hydrogels for promotion of vascular healing. J Biomed Mater Res A. 2004; 68:704–716. [PubMed: 14986325]

22. Nichol JW, Koshy ST, Bae H, Hwang CM, Yamanlar S, Khademhosseini A. Cell-laden microengineered gelatin methacrylate hydrogels. Biomaterials. 2010; 31:5536–44. [PubMed: 20417964]

23. Nikkhah M, Eshak N, Zorlutuna P, Annabi N, Castello M, Kim K, Dolatshahi-Pirouz A, Edalat F, Bae H, Yang Y, Khademhosseini A. Directed endothelial cell morphogenesis in micropatterned gelatin methacrylate hydrogels. Biomaterials. 2012; 33:9009–18. [PubMed: 23018132]
24. Zhao X, Sun X, Yildirimer L, Lang Q, Lin ZY, Zheng R, Zhang Y, Cui W, Annabi N, Khademhosseini A. Cell infiltrative hydrogel fibrous scaffolds for accelerated wound healing. Acta Biomater. 2017; 49:66–77. [PubMed: 27826004]
25. Khayat A, Monteiro N, Smith EE, Pagni S, Zhang W, Khademhosseini A, Yelick PC. GelMA-Encapsulated hDPSCs and HUVECs for Dental Pulp Regeneration. J Dent Res. 2017; 96:192–199. [PubMed: 28106508]
26. Xu X, Chen C, Akiyama K, Chai Y, Le AD, Wang Z, Shi S. Gingivae contain neural-crest-and mesoderm derived mesenchymal stem cells. J Dent Res. 2013; 92:825–32. [PubMed: 23867762]
27. Cha C, Oh J, Kim K, Qiu Y, Joh M, Shin SR, Wang X, Camci-Unal G, Wan KT, Liao R, Khademhosseini A. Microfluidics-assisted fabrication of gelatin-silica core-shell microgels for injectable tissue constructs. Biomacromolecules. 2014; 15:283–90. [PubMed: 24344625]
28. van der Sanden B, Dhobb M, Berger F, Wion D. Optimizing stem cell culture. J Cell Biochem. 2010 Nov.111:801–7. [PubMed: 20803548]
29. Voog J, Jones DL. Stem cells and the niche: A dynamic duo. Cell Stem Cell. 2010; 6:103–115. [PubMed: 20144784]
30. Taqvi S, Dixit L, Roy K. Biomaterial-based notch signaling for the differentiation of hematopoietic stem cells into T cells. J Biomed Mater Res Part A. 2006; 79:689–697.
31. Czyz J, Wobus A. Embryonic stem cell differentiation: the role of extracellular factors. Differentiation. 2001; 68:167–74. [PubMed: 11776469]
32. Shattil SJ, Kim C, Ginsberg MH. The final steps of integrin activation: The end game. Nat Rev Mol Cell Biol. 2010; 11:288–300. [PubMed: 20308986]
33. Moshaverinia A, Xu X, Chen C, Akiyama K, Snead ML, Shi S. Dental mesenchymal stem cells encapsulated in an alginate hydrogel co-delivery microencapsulation system for cartilage regeneration. Acta Biomater. 2013; 9:9343–9350. [PubMed: 23891740]
34. Moshaverinia A, Xu X, Chen C, Ansari S, Zadeh HH, Snead ML, Shi S. Application of stem cells derived from the periodontal ligament or gingival tissue sources for tendon tissue regeneration. Biomaterials. 2014; 35:2642–50. [PubMed: 24397989]
35. Khare AR, Peppas NA. Swelling/deswelling of anionic copolymer gels. Biomaterials. 1995; 16:559–567. [PubMed: 7492721]

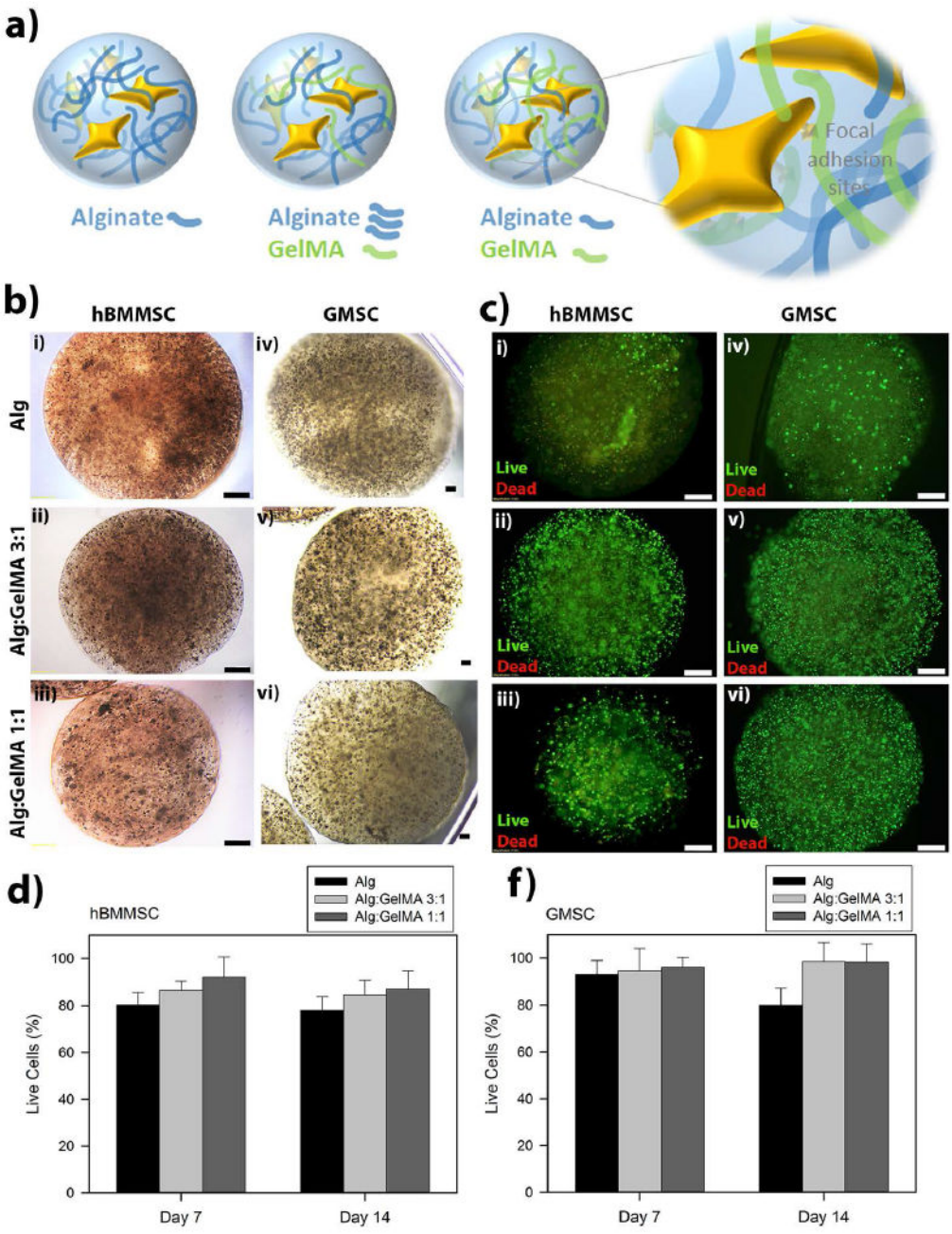

Figure 1. Stem cell encapsulation and viability

(a) Schematic representation of hydrogel microspheres and the hypothesized effect of GelMA presence on cell-biomaterial interactions. (b) Light microscopy images of human bone-marrow mesenchymal stem cell (hBMMSC) (i-iii) and gingival mesenchymal stem cell (GMSC) (iv-vi) loaded hydrogels. Scale bar is 400 μm. (c) Fluorescence images of live/dead cell density inside the designed hydrogel microcapsules. Scale bar is 200 μm. Quantitative live/dead results of encapsulated hBMMSCs (d) and GMSCs (f) inside alginate/GelMA (3:1 and 1:1 w/v%/w/v%) hydrogel microspheres showing the percentage of live cells after one

and two weeks of culturing in regular media. No significant difference was observed in the viability of stem cells encapsulated in the different hydrogels ($p > 0.05$).

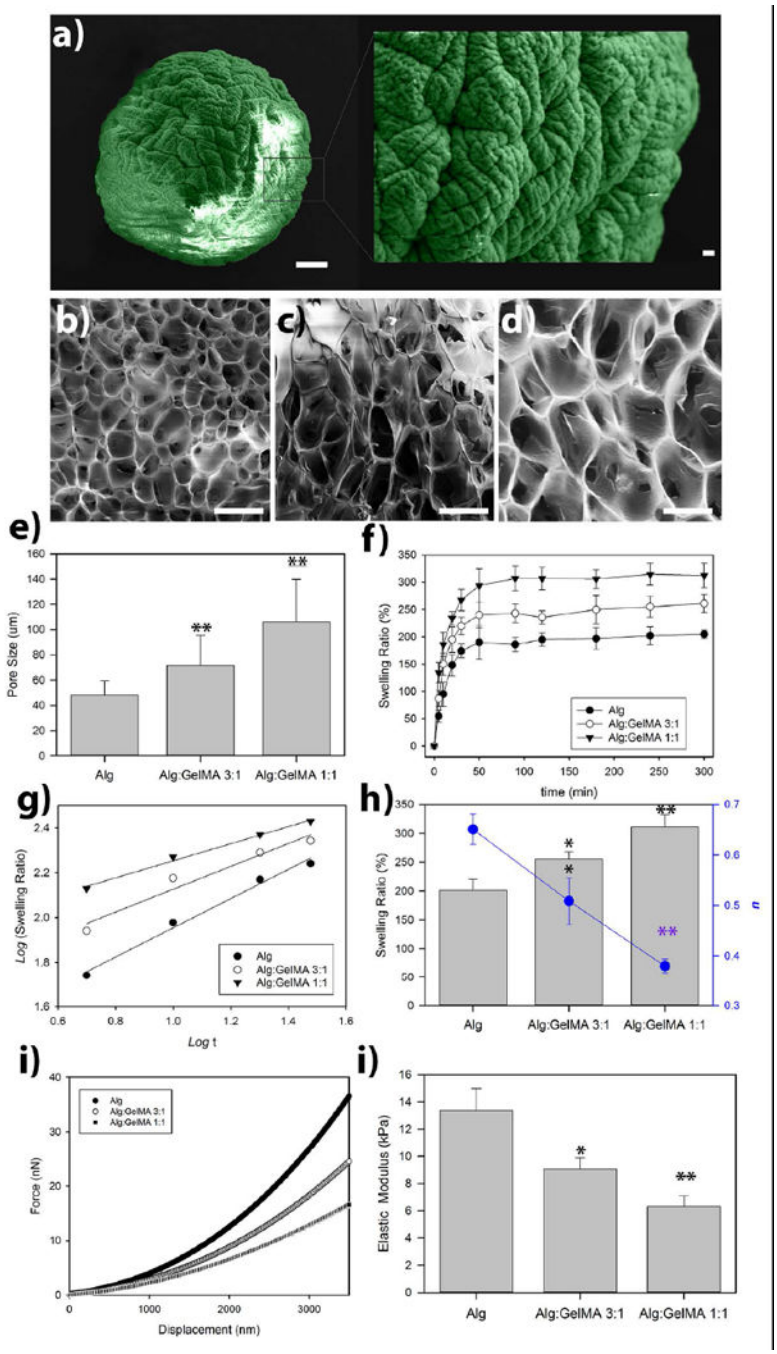

Figure 2. Characterization of the fabricated hydrogels

(a) False-colored scanning electron micrograph of a dried alginate-based microsphere (Alg/GelMA 3:1 w/v%/ w/v%). Scale bar is 100 μm; insert is the magnified view of the sphere (Scale bar is 10 μm). SEM (cross sectional) showing a homogenous macroporous microstructure of freeze-dried alginate (b), alginate/GelMA 3:1 w/v%/ w/v% (c), and alginate/GelMA 1:1 w/v%/ w/v% (d) microspheres. (e) The calculated pore size of the fabricated hydrogel scaffolds. (f) Swelling properties of alginate/GelMA hydrogels were measured at several time points during incubation at PBS buffer at 37°C. (g) Logarithmic

representation of swelling regime. (h) Equilibrium swelling of hydrogels after five days of incubation in PBS buffer at 37°C (bars) and calculated swelling kinetic exponents of hydrogels (blue circles). (i) Force-displacement curves of alginate and alginate/GelMA hydrogel microspheres measured using nanoindentation via atomic force microscopy (AFM). (j) Calculated values of elastic modulus based on Hertz contact mechanics theory. *$p < 0.05$ and **$p < 0.01$.

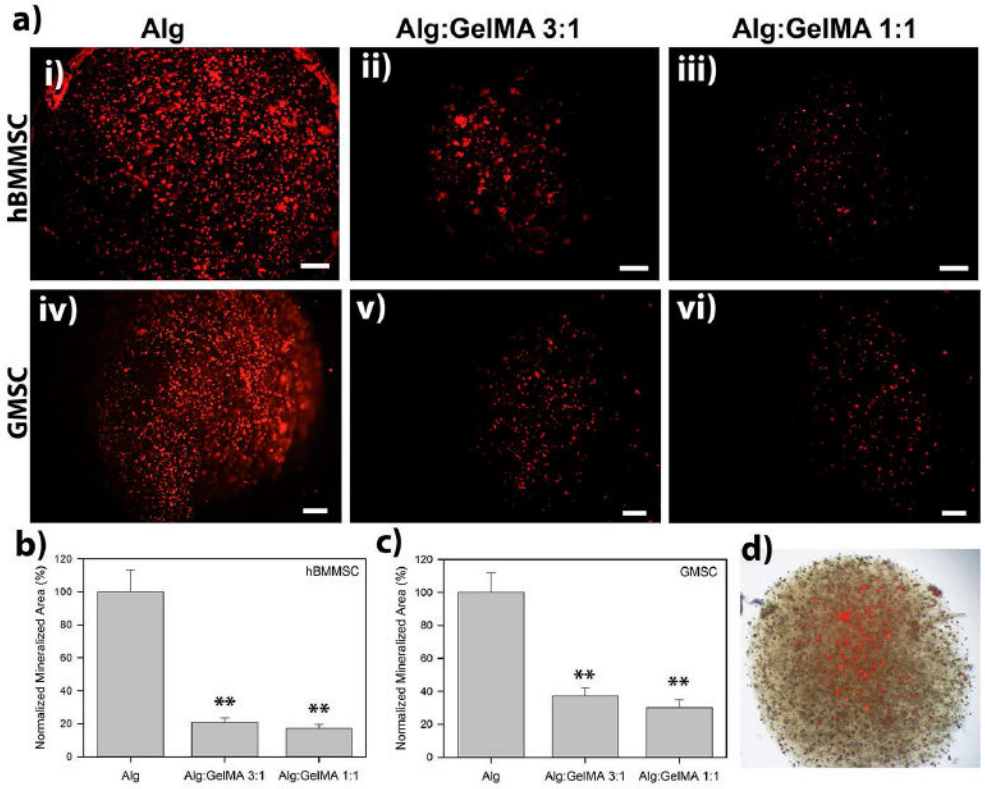

Figure 3. Histochemical analysis of mineralization

(a) Analysis of the mineralization of the encapsulated MSCs after four weeks of culturing in osteogenic medium using xylenol orange (XO). Scale bar is 200 μm. Calculated normalized mineralized area for hBMMSCs (b) and GMSCs (c) encapsulated in alginate/GelMA microspheres with different compositions. (d) Representative light microscopy overlay image of encapsulated stem cells and mineralized regions. *$p < 0.05$ and **$p < 0.01$.

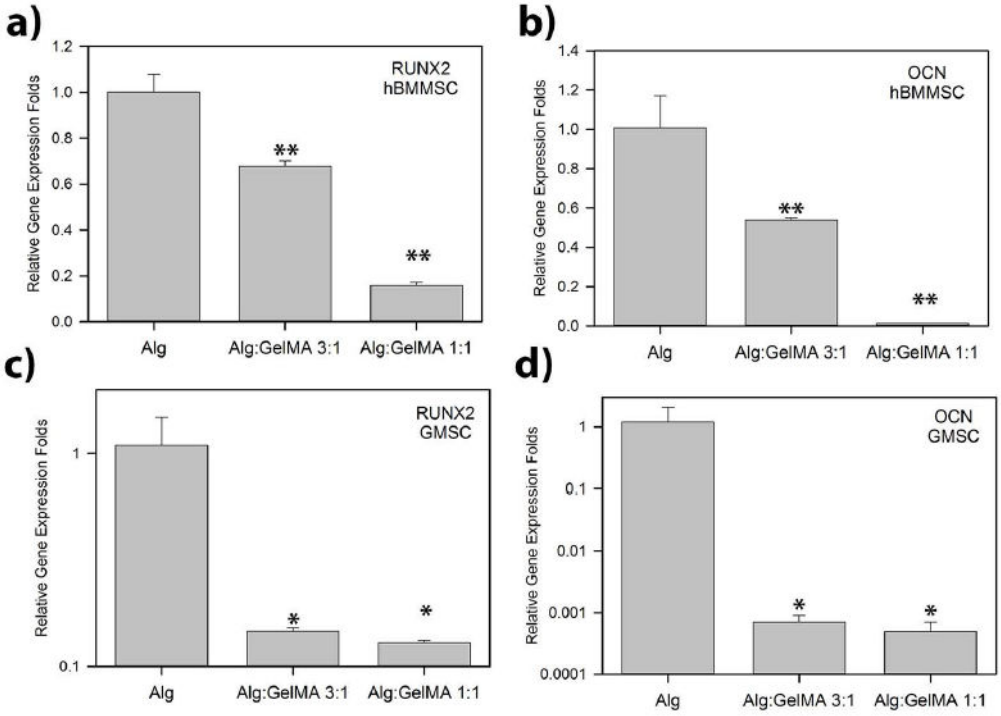

Figure 4. Gene expression analysis of osteogenic markers

PCR analysis of the osteo-differentiation of encapsulated MSCs after four weeks of osteo-differentiation. Expression of two osteo-genes, *RUNX2* and *OCN*, were evaluated with reference to the housekeeping gene *GAPDH*. *$p < 0.05$ and **$p < 0.01$.

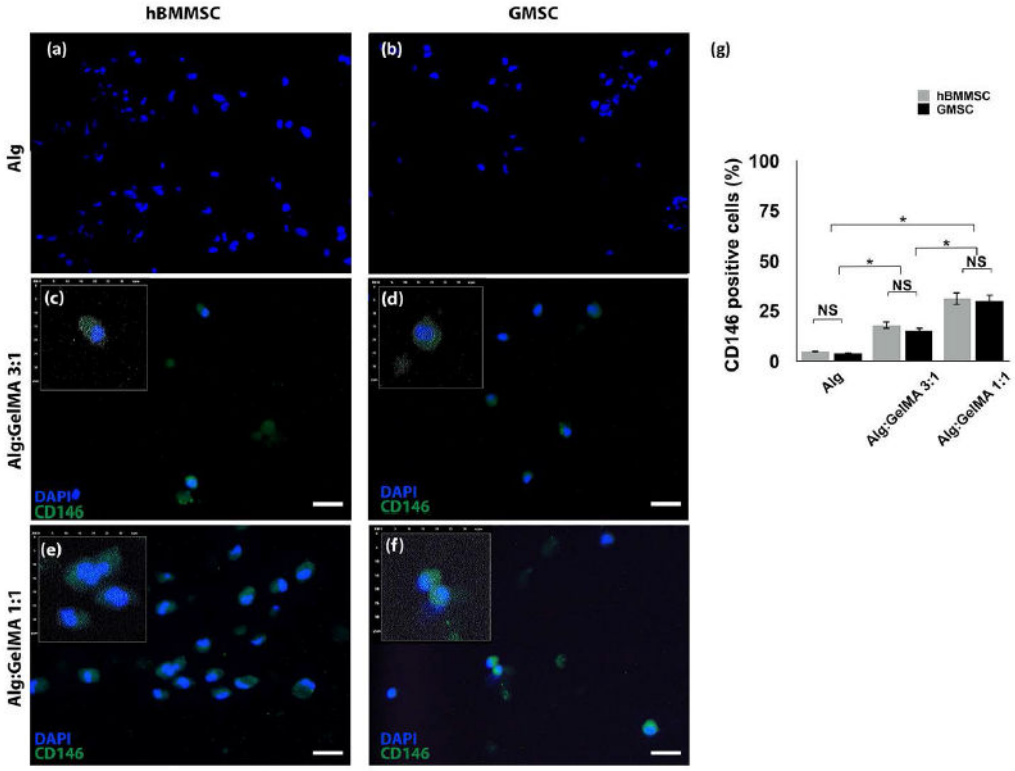

Figure 5. Analysis of the stemness properties of encapsulated MSCs in alginate/GelMA hydrogels

Immunofluorescent microscopy images showing positive staining of encapsulated hBMMSCs (a, c, and e) and GMSCs (b, d, and f) in alginate/GelMA hydrogels after four weeks of osteogenic assay, while MSCs encapsulated in alginate hydrogels failed to present positive staining. Scale bar is 20 μm. Inserts are magnified digitalized images for better demonstration of DAPI (blue) and CD146 (green) pixels, 30×30 μm. (g) Semi-quantitative analysis of positive cells. NS: not significant. *$p < 0.05$.

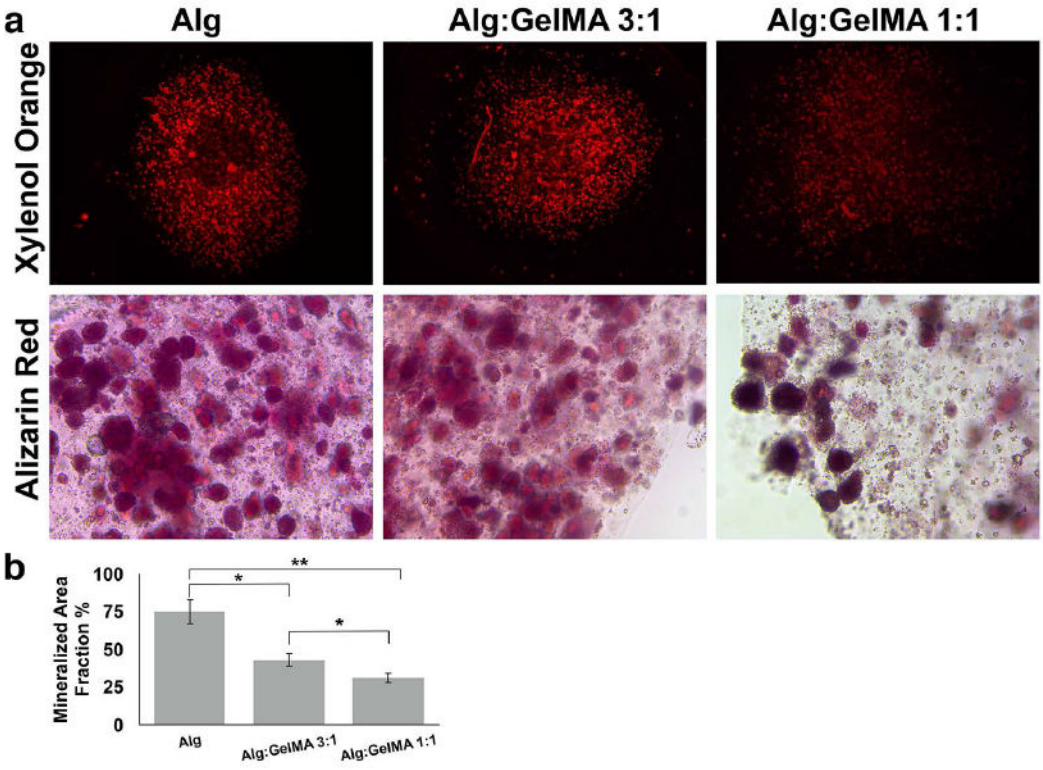

Figure 6. Histochemical analysis of mineralization after rh-BMP-2 treatment

(a) Mineralization analysis of the encapsulated MSCs after four weeks of culturing in medium containing rh-BMP-2 using xylenol orange (XO) and alizarin red (AR) straining. (b) Semi-quantitative analysis of mineralization based on XO staining. NS: not significant. *$p < 0.05$, **$p<0.01$.

Table 1

Oligonucleotide primers used in RT-PCR analysis.

Gene	Sequence	Product (bp)
Runt-related transcription factor 2 (Runx2)	Sense: 5'-CAGTTCCCAAGCATTTCATCC-3'; Antisense: 5'-TCAATATGGTCGCCAAA CAG-3'	289
Osteocalcin (OCN)	Sense: 5'-CATGAGAGCCCTCACA-3'; Antisense: 5'-AGAGCGACACCCTAGAC-3'	292
Peroxisome proliferatoractivated receptor-g2 (PPAR g2)	Sense: 5'-CT CCTATTGACCCAGAAAGC-3'; Antisense: 5'-GTAGAGCTGAGTCTTCTCAG-3'	351
Lipoprotein lipase (LPL)	Sense: 5'-ATGGAGAGCAAAGCCCTGCTC-3'; Antisense, 5'-GTTAGGTCCAGCTGGATCGAG-3'	198
Glyceraldehyde 3-phosphate dehydrogenase (GADPH)	Sense: 5'-AGCCGCATCTTCTTTTGCGTC-3': Antisense: 5'-TCATATTTGGCAGGTTTTT CT-3'	418